

Radar Cross Section Analysis Considering Multi-Reflection inside a Radome Using SBR Method

S. Kuroda*, Y. Inasawa, Y. Konishi, and S. Makino
 Mitsubishi Electric Corporation
 5-1-1 Ohfuna, Kamakura, Kanagawa 247-8501, Japan
 shinkuro@isl.melco.co.jp

1. Introduction

Radar cross section (RCS) for a radome has been studied by using a lot of analysis methods. For example, have been reported the methods based on numerical solutions such as the methods of moments (MoMs) [1]. These methods can analyze effects of multi-reflection inside a radome exactly. However, these methods have to use huge computer memory and huge calculation time when applying large radomes.

In this paper, we propose the simple analysis method based on the shooting and bouncing ray (SBR) method [2] in order to evaluate effects of multi-reflection inside a radome. This method is very simple and it can apply to a large radome RCS analysis at the limited computer condition.

2. Procedure of the Analysis

The shooting and bouncing ray (SBR) method is applied to analyze the RCS of scattering bodies including penetrative object such as radomes. The procedure of the proposed method is as follows;

- (1) The "aperture" is defined around the target as shown in Figure 1 following the SBR roles. The aperture shape and size can be determined arbitrarily.
- (2) Ray tracing is carried out for each incident ray tube from the incident point on the aperture to the plural exit points on the aperture as shown in Fig. 2.
- (3) Surface reflection is only considered for the scattering body.
- (4) Both surface reflection and transmission are applied for the radome.
- (5) Numbers of ray tubes increase one by one when transmitting the radome.

The position \mathbf{P}_0 is determined to be the incident point on the aperture. The positions $\mathbf{P}_1, \mathbf{P}_2, \dots, \mathbf{P}_{n-1}$ are determined to be the reflection and transmission points on the scattering body and the radome. The position \mathbf{P}_n is determined to be the exit point on the aperture. \mathbf{E}_i is assumed to be the electric field of the incident ray tube into the position \mathbf{P}_i . Then, the electric field \mathbf{E}_{i+1} of the incident ray tube into the reflection point \mathbf{P}_{i+1} is described as follows;

$$\mathbf{E}_{i+1} = \mathbf{E}_i \cdot \overline{\overline{\mathbf{R}}}_i \exp(-jk |\mathbf{P}_{i+1} - \mathbf{P}_i|) \quad (1)$$

where $\overline{\overline{\mathbf{R}}}_i$ is a dyadic reflection coefficient at the reflection point \mathbf{P}_i and k is the wave number of the free space.

Also, the electric field \mathbf{E}_{i+1} of the incident ray tube into the transmission point \mathbf{P}_{i+1} is described as follows;

$$\mathbf{E}_{i+1} = \mathbf{E}_i \cdot \overline{\overline{\mathbf{T}}}_i \exp(-jk |\mathbf{P}_{i+1} - \mathbf{P}_i|) \quad (2)$$

where $\overline{\overline{\mathbf{T}}}_i$ is a dyadic transmission coefficient at the transmission point \mathbf{P}_i .

We can obtain the total scattering field by calculating the integration of the electrical field \mathbf{E}_s for each exit ray tube from the aperture and by calculating the summation of all integrations [3],

$$\mathbf{E}_s = \sum_{\substack{\text{All ray} \\ \text{tubes}}} \frac{jk}{4\pi R} \exp(-jkR) \mathbf{S}_e \iint \exp(jk\mathbf{r}' \cdot \hat{\mathbf{o}}) ds' \quad (3)$$

where \mathbf{r}' means a distance between the origin and the point \mathbf{P}_n which is on the aperture plane. \mathbf{S}_e is the

physical quantity relative to electrical and magnetical current at the Pn, which is described using the electrical field on the aperture \mathbf{E}_0 ,

$$\mathbf{S}_e = \hat{\mathbf{o}} \times [(\mathbf{E}_0 \times \hat{\mathbf{o}}) + (\mathbf{E}_0 \times \hat{\mathbf{s}})] \quad (4)$$

where $\hat{\mathbf{o}}$ is the vector direct for the observation point and $\hat{\mathbf{s}}$ is the direction vector of ray tubes.

3. Experiment

We have made the monostatic RCS experiment for the test target to verify the proposed analysis method. Fig. 4 shows configuration of the test target. This is composed of two parts which are the metallic trihedral corner reflector and the regular-triangular dielectric radome plate. The radome aperture is being kept perpendicular to the X axis and the bottom side is parallel to the Y axis. Table 1 denotes electrical characteristics of the radome plate.

Fig. 5 shows frequency characteristics of the monostatic RCS for $\theta = 90$ deg. and $\phi = 0$ deg.. Both the measured and calculated components of the electrical fields are theta components E_θ . The radome aperture of the test target is being kept perpendicular to the ground (X-Y plane). The solid line and dashed line denote the measured and calculated RCS values respectively. The measured value coincides with the calculated value very much.

Fig. 6 denotes the RCS angular pattern at 10 GHz for $\theta = 90$ deg. and $\phi = 0 - 30$ degs.. The solid line and dashed line denote the measured and calculated RCS values respectively. The measured and calculated patterns are in good agreement except for some angle area. The differences in these area seem to be caused by effect of edge diffraction of the metallic corner reflector.

4. Conclusions

The authors proposed the simple analysis method based on the SBR method in order to evaluate effects of multi-reflection inside a radome. Also, the authors confirmed effectiveness of this method by the experiment.

References

- [1] E Arvas and S. Ponnappalli, "Scattering cross section of a small radome of arbitrary shape," IEEE Trans. Antennas and Propagat., vol.37, no.5, pp.655-658, May 1989.
- [2] H. Ling, R. Chou and S. Lee, "Shooting and bouncing rays: Calculating the RCS of an arbitrarily shaped cavity," IEEE Trans. Antennas and Propagat, vol.37, no.2, pp.194-205, Feb. 1989.
- [3] S. W. Lee, H. Ling and R. Chou, "Ray-tube integration in shooting and bouncing ray method," Microwave Optical Tech. Lett., vol.1, pp.286-289, Oct. 1988.

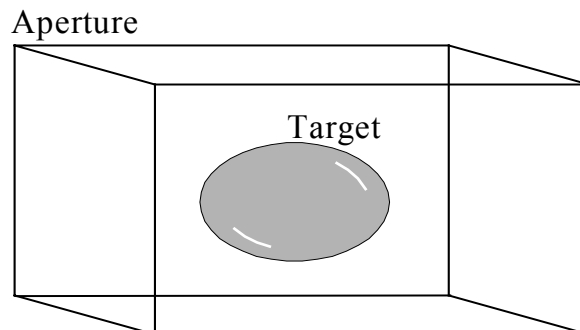


Fig. 1: Aperture and Target.

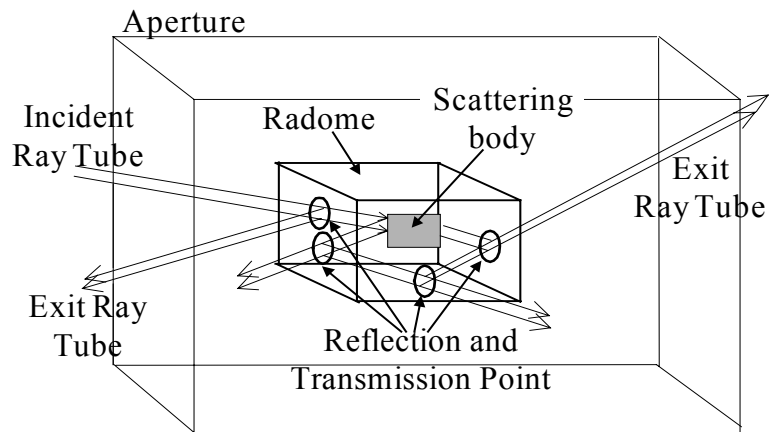


Fig. 2: Ray tracing for one incident ray tube.

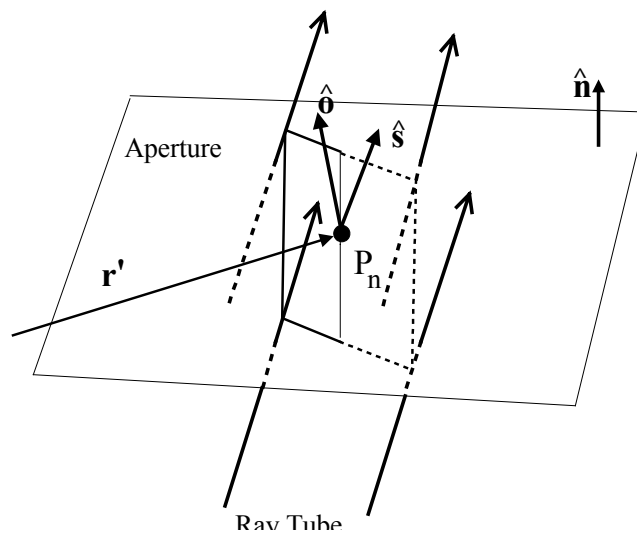


Fig. 3: Ray Tube on the aperture plane.

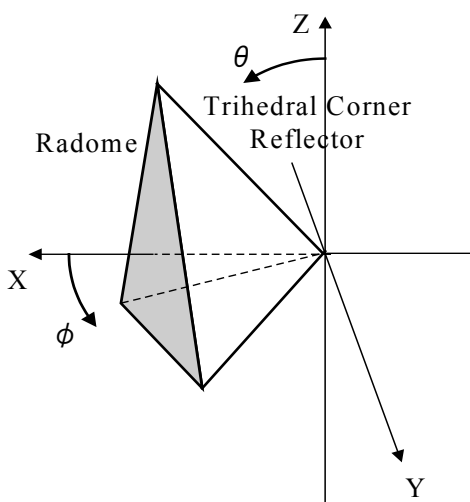


Fig. 4: Test target configuration.

Table. 1: Electrical Characteristics of the radome plate.

Permittivity	3.55
Dissipation Factor	0.003
Thickness	4mm

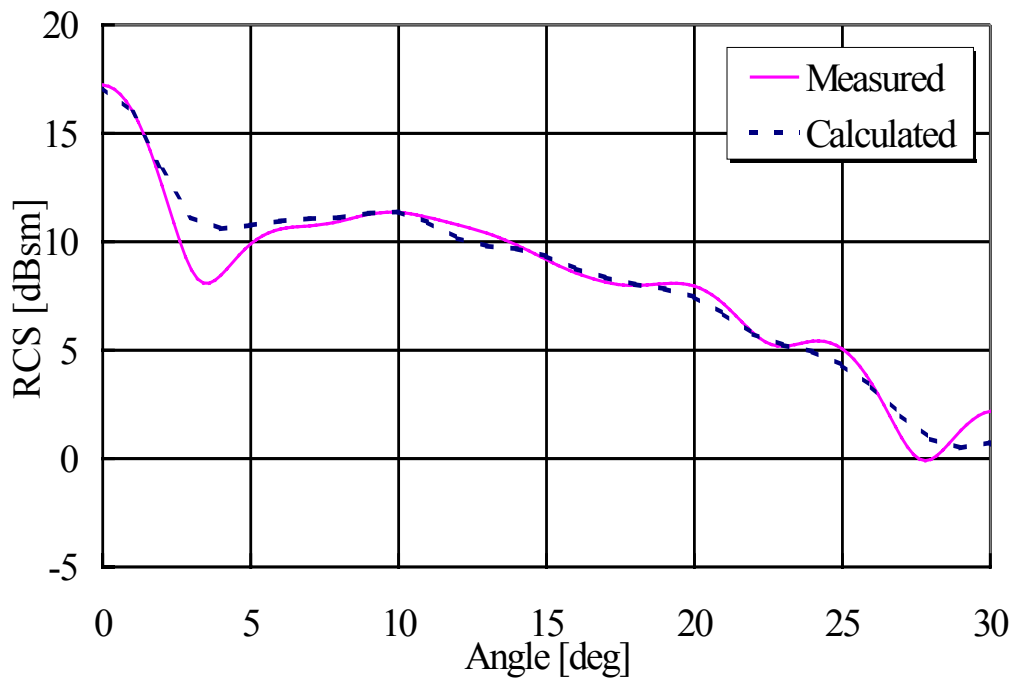


Fig. 5: Frequency characteristics of the RCS (E_{θ} component).

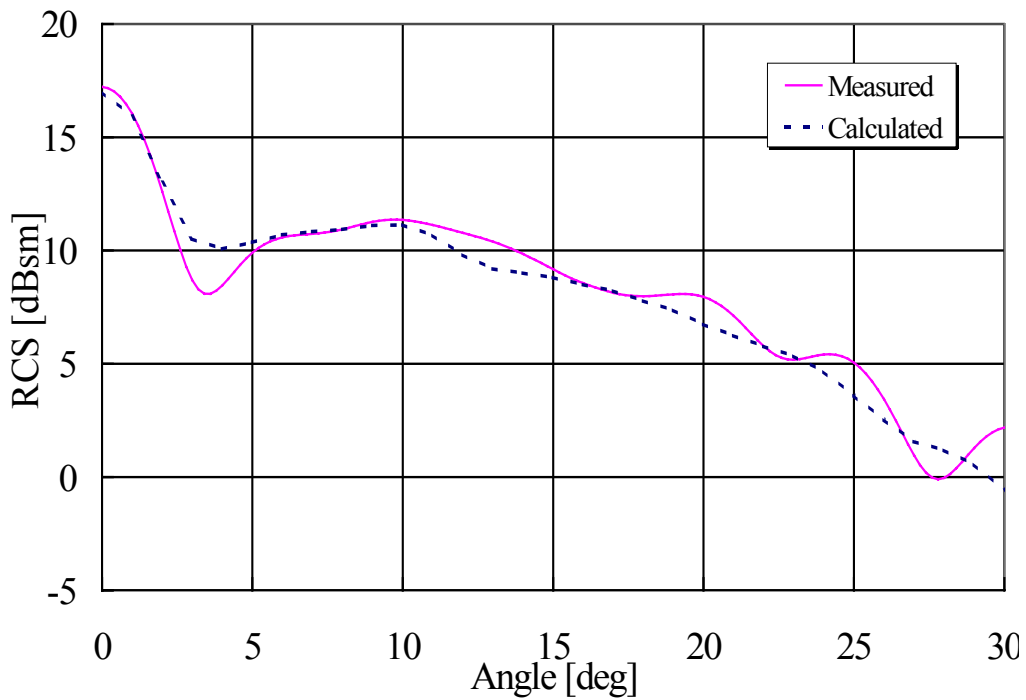


Fig. 6: The RCS angular pattern of the test target at 10GHz (E_{θ} component).